JOURNAL OF OPTOELECTRONICS AND ADVANCED MATERIALS Vol. 9, No. 11, November 2007, p. 3297 - 3302

Proteins adsorption to orthopaedic biomaterials: vibrational spectroscopy evidence

S. CAVALU*, V. SIMON[a]
University of Oradea, Faculty of Medicine and Pharmacy, P-ta 1 Decembrie 10, 410068, Oradea, Romania
[a]Babes-Bolyai University, Faculty of Physics, 400084 Cluj-Napoca, Romania

ATR FTIR spectroscopy and deconvolution techniques are applied in this work in order to obtain structural information on serum albumin and hyaluronidase upon adsorption onto orthopedic biomaterials polymethyl methacrylate. Quantitative analysis of both proteins by curve fitting to the inverted second derivative spectra of the conformationally-sensitive amide I and amide III bands indicate perturbations of both α-helix and β-sheet structures upon adsorption process.

(Received March 23, 2007; accepted November 1, 2007)

Keywords: Orthopaedic biomaterials, Proteins, Vibrational spectroscopy

1. Introduction

Protein adsorption onto medical implants is an essential aspect of the cascade of biological reactions taking place at the interface between synthetic material and biological environment. The type and amounts of adsorbed proteins mediate subsequent adhesion, proliferation and differentiation of cells as well as depositing of mineral phase. Depending on the applications, varying adhesion qualities are demanded: for example bones or tooth implants require good protein adhesion to allow the growth of the bone and formation of a stable and strong interphase between the implants and the bone; in contrast, the protein adhesion has to be poor in temporary contacts with the tissue; for biosensors, the adsorbed proteins or antibodies have to remain biologically active [1-3]. Influences of system parameters on the adsorption mechanisms (such as pH, ionic strength, temperature, izoelectric point of the protein in combination with the material properties such as surface change, electrical conductivity, chemical composition) are not clear or even known. Moreover, shape and conformational changes upon adsorption for varying proteins on different surfaces are mostly unknown. Biocompatibility is dictated by the manner in which the biomaterial surfaces interact with blood constituents (erythrocytes, platelets) as well as the proteins [4,5]. Biocompatible and bioactive materials is a subject of continuous study. New vitroceramic tobe used in reparatory medicine has been obtained and reported in [6]. The biocompatibility towards proteins involves a more complex study. The behavior of a protein at an interface is likely to differ considerably from its behavior in the bulk. Because of the different local environment at the interface, the protein may have the opportunity of adopting a more disordered state exposing its hydrophobic core to the aqueous phase, often called surface denaturation. Denaturation is a process by which hydrogen bonds, hydrophobic interactions and salt linkages are broken and the protein is unfolded. The denaturation of secondary structure involves also changes in ratio among the three common structures: α helix, β sheets or turns and unordered. The physical changes that occur when a solution of globular proteins is heated have been investigated extensively and two distinct transitions can be identified: initially, the protein molecules undergo a change in conformation as a cooperative transition to a more open, less structured state (unfolding), characterized by an increase in the viscosity of the solution, followed by the onset of intermolecular association or aggregation of individual unfolded protein molecules, this process being accompanied by divergence in viscosity and development of gelation [7].

FTIR spectroscopy which can be used to study protein secondary structure in any state (i.e. aqueous, frozen, dried or even as an insoluble aggregate) is one of the most used techniques for studying stress induced alterations in protein conformation and for quantifying protein secondary structure. Hence, ATR-FTIR can provide important information leading to the development of novel biomaterials as replacements for damaged or diseased natural tissue. The spectral region of amide I (1660 cm^{-1}), amide II (1550 cm^{-1}) and amide III (1300cm^{-1}) are very sensitive to the conformational changes in the secondary structure of proteins. Computational techniques based on the second derivative spectra and deconvolution procedure is used for percentage evaluation of each secondary structure and also the perturbations upon the adsorption to different surfaces [7-10].

According to literature, the prior deposition of a thin protein film onto the biomaterial surface can be favorable to the development of the new bone [11-13]. These organic molecules may either completely envelope or themselves be enveloped by the mineral crystals. They are essential for the initial deposition of mineral crystals because they may serve as seeds for crystallization and possibly influence the number of nucleation sites generated and also their subsequent grown , orientation and organization.

2. Experimental

The lyophilized proteins (bovine serum albumin MW=66 kDa and hyaluronidase from bovine testes, type VII, MW=55 kDa) were obtained from Sigma and used without further purification. The proteins were rehydrated in phosphate buffer physiological saline (pH=7.5) at a final concentration of 35 mg/ml and 3 mg/ml respectively for BSA and hyaluronidase. PMMA (polymethyl methacrylate) bone substitute was purchased from Stryker Howmedica Osteonics, commercially available as BIOLOS3® and ANTIBIOTIC SIMPLEX®. The major difference between these two materials is the antibiotic presence in SIMPLEX- erythromycin and colystin [14] After polymerization, small plates of PMMA were incubated for 24 hours at 37 °C in both protein solution and, after drying process, the surfaces were analyzed by ATR FTIR spectroscopy.

The FT-IR spectra of lyophilized proteins were recorded in the region 4000-800 cm^{-1} by a Bruker EQUINOX 55 spectrometer OPUS software, using an Attenuated Total Reflectance accessory with a scanning speed of 32 cm^{-1} min^{-1} with the spectral width 2.0 cm^{-1}. The internal reflection element was a ZnSe ATR plate (50 × 20 × 2 mm) with an aperture angle of 45°. A total of 128 scans were accumulated for each spectrum.

Spectra were recorded at a nominal resolution of 2 cm^{-1}. The resultant spectra were smoothed with a 9-point Savitsky–Golay smooth function to remove the white noise. The second derivative spectral analysis was applied to locate positions and assign them to different functional groups . Before starting the fitting procedure, the obtained depths of the minima in the second derivative spectrum and, subsequently, the calculated maximum intensities were corrected for the interference of all neighbouring peaks. All second-derivative spectra, calculated with the derivative function of Opus software, were baseline-corrected, based on the method of Dong and Caughey [15], and area-normalized under the second derivative amide I region, 1700–1600 cm^{-1} and amide III region, 1330-1230 cm^{-1} .

The curve fitting is performed by stepwise iterative adjustment towards a minimum root-mean-square error of the different parameters determining the shape and position of the absorption peaks. Curve fitting was performed by setting the number of component bands found by second-derivative analysis with fixed bandwidth (12 cm^{-1} for amide I and 14 cm^{-1} for amide III) and Gaussian profile. The best-average fit gave the intensity of each component band for each spectrum. The area under each peak was used to calculate the percentage of each component and, finally, to analyze the percentage of secondary structure component.

3. Results and discussion

Albumin was selected as a representative protein for study because it is the most abundant protein in mammalian blood plasma (concentration ranging from 30 to 55 mg/ml). Thus, the possibility of albumin adsorbing on an implant surface should be higher than for other less concentrated proteins present in body fluid. On the other hand, the hyaluronic acid is an important constituent of extracelular matrix of vertebrates. Hyaluronidase hydrolyzes the endo-N-acetylhexosaminic bonds of hyaluronic acid (HA) and chondroitin sulfuric acids A and C (but not B), primarily to tetrasaccharide residues [16]. Recently [17] it has been demonstrated the possibility that elevated levels of HA/HAase could be a marker for prostate cancer progression based on their understanding that many tumors share similar characteristics of growth and metastasis.

The ATR FTIR spectra of free lyophilized albumin and albumin adsorbed to PMMA-based biomaterials (SIMPLEX® and BIOLOS3®, respectively) after 24 h incubation, are shown in Fig. 1 (a, b, c).

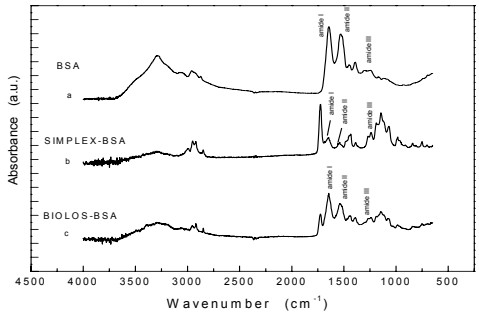

Fig. 1. ATR-FTIR spectra of lyophilized free albumin (a) and after adsorption to SIMPLEX® (b) and BIOLOS® (c) orthopedic biomaterials.

The amide I band, located between 1700 and 1600 cm^{-1} is composed mainly (around 80%) of the C=O stretching vibration of the peptidic bond and amide II vibrations derives mainly from in plane N-H bending (40-60%), the C-N (18-40%) and C-C (10%) stretching vibrations located between 1530-1560 cm^{-1}. Amide III (between 1220 and 1320 cm^{-1}) is a more complex vibrational mode. It mainly is the in-phase combination of NH in-plane-bending and CN stretching with contributions from CC stretching and CO in-plane-bending, depending on the details of the force field, the nature of side chains and hydrogen bonding. Other bands in Fig. 1(b,c) indicate the details of functional groups in polymethyl methacrylate; a sharp and intense band at 1726 $cm^{-1}$is due to the presence of ester carbonyl group stretching mode, a broad band at 1438 cm^{-1} due to C-H bending and the peaks in the range 1260-900 cm^{-1} are assigned to O-C-O, C-CH_3 stretching and C-COO vibrations. According to literature [18,19], as a general behavior, the shift of amide I to higher numbers after adsorption, indicates a modification of the secondary structure, while a decreased intensity of the amide II band suggests an increased accessibility of amide bond to water. As a quantitative aspect, BIOLOS has obviously a higher capability to adsorb albumin, as the intensity of amide I

and II bands are more intense compared to albumin adsorbed to SIMPLEX® biomaterial.

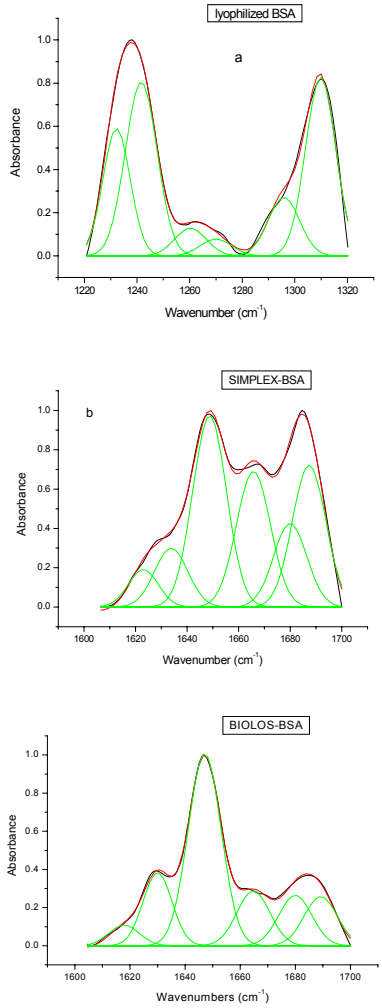

Fig.2. Deconvolution of amide I spectral region of lyophilized free albumin (a) and adsorbed to SIMPLEX® (b) and BIOLOS® (c).

Each type of secondary structure (i.e. α-helix, β-sheet, β-turn and unordered) gives rise to different C=O stretching frequencies [7-10,20], and hence, results in characteristic band positions. Band positions are used to determine the individual component of secondary structure. The relative band areas (determined by curve fitting) can then be used to quantitate the relative amount of each structural component. Fig. 2(a,b,c) show the inverted second derivative amide I spectra of the free serum albumin lyophilized (Fig. 2a) and adsorbed to both biomaterials (Fig. 2b,c). Assignments of the bands in Table I was made on the basis of previous reported studies, along with the quantitative analysis. Fourier deconvolution, used to determine the component band positions, reveals that the band in range 1650-1662 cm^{-1} is characteristic of α-helical structures. The bands in the region 1630-1640 cm^{-1} are characteristic for native β-sheet structures, the bands around 1645 cm^{-1} are correlated to the unordered structures, while the bands in the range 1680-1690 cm^{-1} may possibly be attributed to β-turns [1-3,7]. On the basis of earlier IR studies [7], the bands around 1620 cm^{-1} are indicative of intermolecular (antiparallel) β sheet and according to literature, is a common IR spectral features for both lyophilization and temperature-induced protein aggregation. It was suggested that the aggregation was formed from partially unfolded protein molecules, through the cross-linking of intermolecular β-sheet structures, as a result of the exposure of hydrophobic residues [21, 22].

The same analysis by second derivative and Gaussian curve fitting were made for the amide III region (Fig. 3 a,b,c) the results being listed in Table 2 along with the assignments.

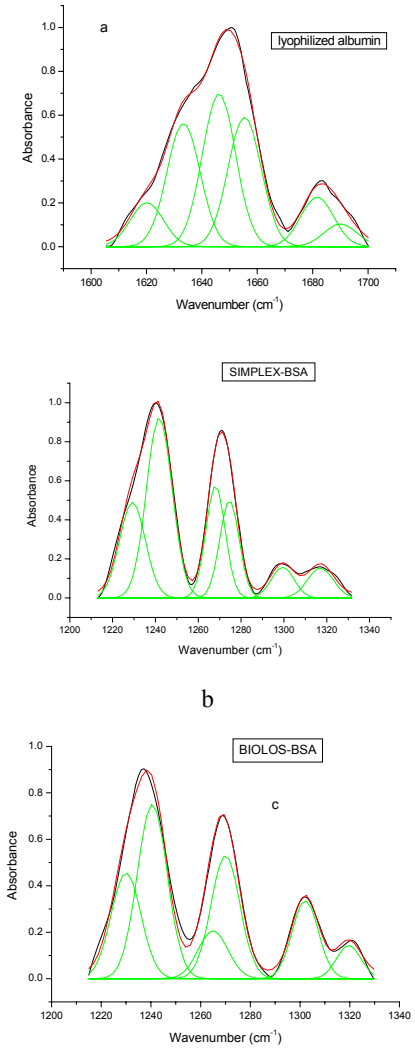

Fig.3. Deconvolution of amide III spectral region of lyophilized free albumin (a) and adsorbed to SIMPLEX® (b) and BIOLOS® (c)

In concordance with the amide I calculations, the α-helical and β-sheet structures show a decreased content upon adsorption to biomaterials, concomitant to the increasing concentration of β-turns. The small changes in the quantitative amount of secondary structure

components upon adsorption to different PMMA-based biomaterials can be interpret as a consequence of different states of hydratation of the adsorbed protein. PMMA is considered to be a hydrophilic surface, but upon the antibiotic loading procedure (in the case of SIMPLEX®) the surface properties are affected and albumin undergoes different unfolding compared to the similar surface, BIOLOS®.

Table 1. Assignments and relative areas of amide I components of lyophilized free albumin and adsorbed albumin to orthopedic biomaterials.

Amide I	β sheet intermolecular	β sheet native	unordered	α helix	turns	turns
	ν(cm^{-1}), A%	ν(cm^{-1}), A%	ν(cm^{-1}), A%	ν(cm^{-1}), A%	ν(cm^{-1}), A%	ν(cm^{-1}), A%
Free BSA lyophilized	1620 8.4%	1633 22%	1648 29%	1658 26%	1681 10.3%	1690 4%
SIMPLEX-BSA	1623 5%	1633 9%	1648 30%	1662 21%	1681 13%	1687 22%
BIOLOS-BSA	1618 4.5%	1630 15%	1647 44%	1662 13%	1680 12%	1689 11.5%

Table 2. Assignments and relative areas of amide III components of lyophilized albumin and adsorbed albumin to orthopedic biomaterials.

Amide III	β sheet	unordered	turns	turns	α helix	α helix
	ν(cm^{-1}), A%	ν(cm^{-1}), A%	ν(cm^{-1}), A%	ν(cm^{-1}), A%	ν(cm^{-1}), A%	ν(cm^{-1}), A%
Free BSA lyophilized	1232 24%	1241 34%	1260 6%	1270 4%	1295 7%	1309 25%
SIMPLEX-BSA	1229 18%	1241 34%	1268 17%	1278 14%	1299 8%	1316 8.5%
BIOLOS-BSA	1230 19%	1240 32%	1264 9%	1273 22%	1302 13%	1319 5%

The adsorption properties of PMMA-based biomaterial (BIOLOS3®) were further investigated with respect to hyaluronidase. The ATR FTIR spectra of this enzyme, lyophilized, is presented in Fig. 4 and the adsorption of hyaluronidase to BIOLOS surface after incubation is emphasized in Fig. 5(a,b) by the amide I band at 1646 cm^{-1}, amide II at 1545 cm^{-1} and amide III band centered at 1280 cm^{-1}. Fourier deconvolution of amide I and III as well as band fitting procedure were performed in order to obtain more qualitative and quantitative information related to the adsorption induced conformational transitions.

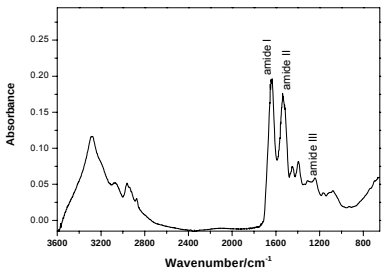

Fig. 4. *ATR- FT-IR spectrum of hyaluronidase (lyophilized powder).*

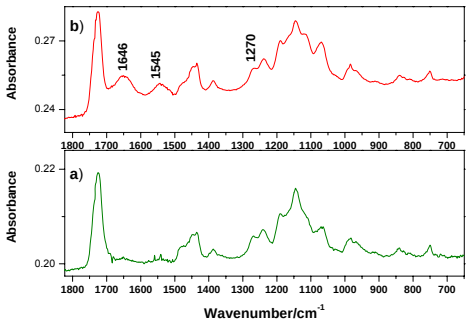

Fig. 5. a) ATR-FT-IR spectra of BIOLOS® surface, b) Hyaluronidase adsorbed to BIOLOS® surface after 24 h incubation.

Fig. 6 shows the deconvolution of amide I band of the native (a) and adsorbed enzyme (b) on BIOLOS® surface. The individual components of amide I native enzyme (table 3) are related to α helix structure (1648 cm^{-1}), β sheet (1631 cm^{-1}), turns (1661 -1685 cm^{-1}) and aggregates from β sheet-intermolecular (1619 cm^{-1}). The related components of the adsorbed enzyme are shifted toward higher wavenumbers and the percentage area of each component is changed. The α helix content decreased from 32.2% to 27.5% upon adsorption; β sheet decrease also

from 35.5% to 18.% accompanied by an increase of β-turns structure from 24% to 42.3 % and the aggregates from 8% to 11%.

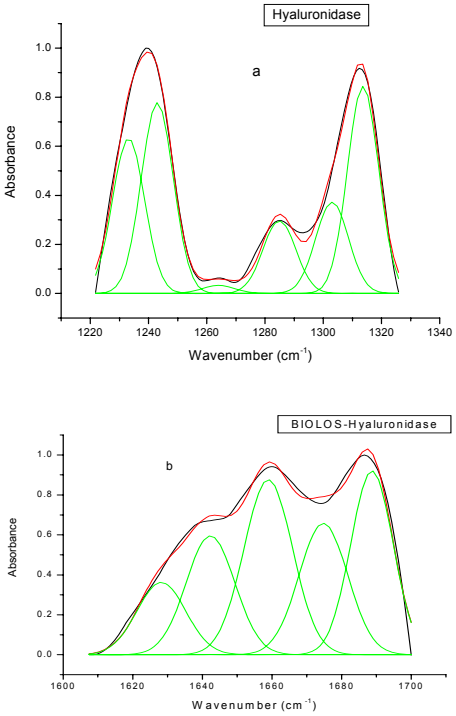

Fig.6. Deconvolution of amide I spectral region of lyophilized free hyaluronidase (a) and adsorbed to BIOLOS® (b) .

The amide III deconvolution (Fig. 7) and quantitative analysis (Table 4) is in concordance with the amide I calculations emphasizing perturbations related to the percentage of each component (but not related to the band position), the α helix spectral region being obviously affected, as supported by the visual inspection of the bands in Fig. 6.

Comparing the results from both proteins, one can observe that hyaluronidase appear to be more susceptible to conformational changes due to the adsorption process, since spectral alterations reflected on intermolecular β - sheet (protein aggregates), β- turns and α helix content are more obvious as compared with serum albumin.

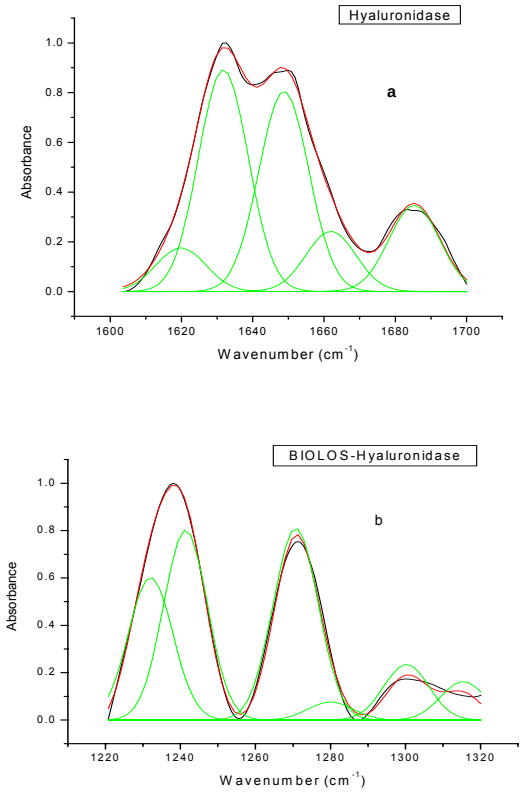

Fig.7. Deconvolution of amide III spectral region of lyophilized free hyaluronidase (a) and adsorbed to BIOLOS® (b).

Table 3. Assignments and relative areas of amide I components of lyophilized free hyaluronidase and adsorbed to orthopedic BIOLOS® material.

Amide I	β sheet intermolecular	β sheet native	α helix	turns	turns
	ν(cm^{-1}), A%	ν(cm^{-1}), A%	ν(cm^{-1}), A%	ν(cm^{-1}), A%	ν(cm^{-1}), A%
Free hyal. lyophilized	1619 8%	1630 35.5%	1650 32.2%	1661 10%	1685 14%
BIOLOS-hyal.	1628 11.5%	1640 18.5%	1658 27.5%	1674 20.6%	1688 21.7%

Table 4. Assignments and relative areas of amide III components of lyophilized hyaluronidase and adsorbed to orthopedic biomaterials.

Amide III	β sheet	unordered	turns	turns	α helix	α helix
	ν(cm^{-1}), A%	ν(cm^{-1}), A%	ν(cm^{-1}), A%	ν(cm^{-1}), A%	ν(cm^{-1}), A%	ν(cm^{-1}), A%
Free hyal. lyophilized	1233 22.7%	1243 26%	1264 1.3%	1280 10%	1303 13.5%	1313 27%
BIOLOS-hyal.	1232 21.3%	1241 29%	1270 31%	1280 3.2%	1300 8%	1315 7%

4. Conclusions

Second derivative amide I and amide III infrared spectra can be used to investigate changes in secondary structure of serum albumin and hyaluronidase during the adsorption processes on to orthopedic biomaterials (PMMA) which involves their denaturation. Simultaneous qualitative and quantitative analysis of amide I and amide III features by deconvolution and curve fitting to the inverted second derivative spectra reveals a decrease in α-helix and β-sheet content, concomitant to the increasing concentration of β-turns, for both proteins, but the evidence of these changes is more obvious in the case of hyaluronidase.

Acknowledgements

This study was supported by MATNANTECH-CEEX grant nr. 100/2006.

References

[1] K. Rezwan, L.P. Meier, L.J. Gaukler, Biomaterials, **26**, 4351 (2005).
[2] A. Dong, J.D. Meyer, J.L. Brown, M.C. Manning, J.F. Carpenter, Arch. Biochem. Biophys. **383**, 148 (2000).
[3] M.Van de Weert, P. I. Haris, W. E. Hennink, D. J. A. Crommelin, Anal.Biochem. **297,**160(2001).
[4] W. Aken, Steen Dawis ed., Kluwer academic publishers, Norwell, Massachusetts, USA, 1989.
[5] K. Vijayanand, D. K. Pattanayak, T. R. Rama Mohan, R. Banerjee, Trends Biomater. Artif. Organs **18** (2),73 (2005).
[6] C. Mazilu, L. Ionescu, E. Rotiu, A. Dimischiotu, A. Campean, J. Optoelectron. Adv. Mater. **8**(2), 741 (2006).
[7] A. Dong, S.J. Prestrelski, S.D. Allison, J.F. Carpenter, J. Pharm. Sci. **84** , 415 (1995).
[8] D. M. Byler, H. Susi, Biopolymers **25**, 469 (1986).
[9] H. Susi, D.M. Byler, Methods Enzymol. **130**, 290 (1986).
[10] W. K. Surewicz, H. H. Mantsch, Biochim. Biophys. Acta **953**, 115 (1988).
[11] L. Pramatarova, E. Pecheva, R. Presker, M.T. Pham, M.F. Maitz, M. Stutzmann, Eur.Cells Mater. **9**, 9 (2005).
[12] J. Xie, C. Riley, M.Kumar, K.Chittur, Biomaterials **23**, 3609(2002).
[13] E. Fujii, M. Ohkubo, K.Tsuru, S. Hayakawa, A.Osaka, K, Kawabata, C.Bonhomme, F. Babonneau, Acta Biomater.**2**, 69 (2006).
[14] S. Cavalu, V. Simon, JOAM **8**(4**)**, 1520 (2006).
[15] A.Dong, W.S. Caughey, Methods Enzymol**.** **232**, 139 (1994).
[16] V. B. Lokeshwar, G. L. Schroeder, R. I. Carey, M. S. Soloway, N. Iida, Biol. Chem **277**, 37, 33654 (2002).
[17] J. T. Posey, M.S. Soloway, S.Ekici, Cancer Res**.** **63**, 2638 (2003).
[18] J. Xie, C. Riley, M. Kumar, K Chittur, Biomaterials **23**, 3609 (2002).
[19] A. W. P. Vermer, Conformations of adsorbed proteins, in Enciclopedia of Surface and Colloid Science, Dekker Encyclopedias, Taylor and Francis (2002), 1193.
[20] H. H. Mantsch, D. Chapman, Infrared Spectroscopy of Biomolecules, Wiley-Liss, New York.
[21] A. Kato, T.Takagi, J. Agric. Food Chem **36**, 1156 (1988).
[22] K. Griebenow, A. M. Klibanov, Proc.Nat. Acad. Sci. USA 92, Nov. (1995).

*Corresponding author: scavalu@rdslink.ro